^{13}C MAS NMR Studies of Crystalline Cholesterol and Lipid Mixtures Modeling Atherosclerotic Plaques

Wen Guo and James A. Hamilton
Department of Biophysics, Boston University School of Medicine, Boston, Massachusetts 02118 USA

ABSTRACT Cholesterol and cholesteryl esters are the predominant lipids of atherosclerotic plaques. To provide fundamental data for the quantitative study of plaque lipids in situ, crystalline cholesterol (CHOL) and CHOL/cholesteryl ester (CE) mixtures with other lipids were studied by solid-state nuclear magnetic resonance with magic-angle-sample spinning. Highly distinctive spectra for three different crystalline structures of CHOL were obtained. When CHOL crystals were mixed with isotropic CE oil, solubilized CHOL (~13 mol % CHOL) was detected by characteristic resonances such as C5, C6, and C3; the excess crystalline CHOL (either anhydrous or monohydrate) remained in its original crystalline structure, without being affected by the coexisting CE. By use of ^{13}C-enriched CHOL, the solubility of CHOL in the CE liquid-crystalline phase (~8 mol %) was measured. When phosphatidylcholine was hydrated in presence of CHOL and CE, magic-angle-sampling nuclear magnetic resonance revealed liquid-crystalline CHOL/phosphatidylcholine multilayers with approximately an equal molar ratio of CHOL/phosphatidylcholine. Excess CHOL existed in the monohydrate crystalline form, and CE in separate oil or crystalline phases, depending on the temperature. The magic-angle-sampling nuclear magnetic resonance protocol for identifying different lipid phases was applied to intact (ex vivo) atherosclerotic plaques of cholesterol-fed rabbits. Liquid, liquid-crystalline, and solid phases of CE were characterized.

INTRODUCTION

Ischemic heart disease is a major cause of death and disability in many societies. The primary cause of heart disease as well as of ischemic damage to the brain and other organs is atherosclerosis, which results in narrowing of blood vessels that feed these tissues. Although atherosclerosis is a complex process that may have many causes, it is always characterized by accumulation of lipids, mainly crystalline cholesterol (CHOL) and CHOL/cholesteryl ester (CE), in the intimal layers of vessels (Small, 1988). Knowledge of the composition and physical chemistry of atherosclerotic plaques is essential for understanding how these plaques originate and mature and how reversal of the pathological process may be achieved (Small, 1988). It is therefore important to develop new techniques to characterize more completely the chemical and physical aspects of atheroslerosis.

Physical techniques such as differential scanning calorimetry, optical and electron microscopy, and x-ray diffraction provide specific data on certain aspects of the physical chemistry of plaque lipids (Small, 1988). In general, these methods do not directly identify the molecular species that give rise to the physical observation. Newer methods such as micro-Fourier-transform IR spectroscopy give information about some chemical constituents, especially CE, and their concentrations in plaques (Kodali et al., 1991). Standard high-resolution ^{13}C nuclear magnetic resonance (NMR) spectroscopy can yield chemical, in addition to physical, information (Hamilton et al., 1979; Kroon et al., 1982; Toussaint et al., 1994); however, detailed data are obtained only for the liquid phase, and solid phases are not detected. By use of solid-state ^{13}C NMR with magic-angle-sample spinning (MAS), it is possible to obtain high-resolution spectra of liquid-crystalline and crystalline phases. Polycrystalline lipids that have crystal structures with symmetrically inequivalent molecules exhibit distinguishable peaks for the same carbon nuclei at different crystallographic sites (Guo and Hamilton, 1993, 1995a,b). MAS NMR can be used to monitor the phase transitions, to detect all the coexisting phases in mixtures of CE with different acyl chains, and to determine the crystal structure of CE (Guo and Hamilton, 1995a). In principle, it can provide information about the structural organization, molecular motions, and chemical composition in more-complex mixtures and biological samples.

To complete our development of MAS NMR approaches for detection of lipids in plaques, we have studied pure CHOL and mixtures of lipids that model plaque lipids by ^{13}C MAS NMR. CHOL is a major constituent of plaques and exists primarily in a crystalline form in mature plaques. Following characterization of CHOL in its hydrated and anhydrous forms, we examined in detail the interactions of CHOL and CE in lipid mixtures of increasing complexity. We show that ^{13}C MAS NMR provides the most comprehensive physical and chemical description of such lipid mixtures to date. Finally, we applied our MAS NMR protocol to the identification of lipids in an atherosclerotic lesion from a New Zealand White rabbit artery. These results demonstrated that MAS NMR permits a detailed, nondestructive analysis of intact excised atherosclerotic plaques.

Received for publication 21 May 1996 and in final form 31 July 1996.

Address reprint requests to Dr. James A. Hamilton, Department of Biophysics, Boston University School of Medicine, Center for Advanced Biomedical Research W302, 80 East Concord Street, Boston, MA 02118-2394. Tel.: 617–638-5048; Fax: 617-638-4041; E-mail: hamilton@med-biophd.bu.edu.

0006-3495/96/11/2857/12 $2.00

EXPERIMENTAL

Materials

CHOL, CE [cholesteryl palmitate (CP), cholesteryl oleate (CO), cholesteryl linoleate (CL)] and triolein (TO) were purchased from Nu-Chek Prep (>99% pure; Elisian, MN). Egg phosphatidylcholine (eggPC) and 1,2-dipalmitoyl-*sn*-3-glycero-phosphocholine (DPPC) were purchased from Avanti Polar Lipids (>99% pure; Alabaster, AL). The impurity contents of TO, CE, eggPC, and DPPC were confirmed by TLC to be <2-3%, and the lipids were used as received. After NMR experiments, lipid mixtures were examined by TLC, and there was no significant increase in the impurity content for CHOL, CE, TO, and DPPC. However, eggPC degraded significantly (10–15%) after prolonged data acquisition at elevated temperature, and in these cases DPPC was substituted for eggPC.

Anhydrous CHOL was recrystallized from dry ethanol, and trace amounts of ethanol were removed under vacuum for 24 h. We obtained CHOL monohydrate (ChM) by first dissolving CHOL in pure ethanol and then adding deionized water drop by drop until a white precipitate appeared. The resulting suspension was heated in a water bath until a clear solution appeared. This process was repeated until the heating no longer dissolved the precipitate; we then added a drop of ethanol to retain a clear solution, which was allowed to cool gradually to room temperature. The final solution, usually containing ~30% water by volume, was stored at 4°C. After crystallization, the solid was soaked in a large quantity of cold deionized water to remove the residual ethanol. The supernatant water was replaced three times, and the solid was then stored in water at 4°C before use. The various crystalline forms were confirmed by their thermal phase transitions detected by differential scanning calorimetry and by their characteristic x-ray powder diffraction pattern (Small, 1986).

Sample preparation

Anhydrous CHOL (ChA) was ground into a powder and loaded into the MAS NMR sample rotor directly. The ChM was ground under water and loaded into the rotor in the presence of excess water. A CE mixture of CO/CP/CL (69:17:14 wt %) was prepared to model the lipid deposit of CHOL-fed rabbit artery (see below); the phase behavior of this mixture has been presented elsewhere (Guo and Hamilton, 1995a). This CE mixture is used throughout the study reported here unless otherwise mentioned. We prepared ChA/CE and ChM/CE mixtures by weighing the desired amount of each component and mixing the components either at a temperature above the CE melting point or in $CHCl_3$ solution followed by drying under vacuum for 12 h. Samples containing ChM were prepared in the presence of excess water. We prepared a mixture of ChA, CE, and eggPC or DPPC by mixing the desired amount of each component in $CHCl_3$, forming a thin film under N_2, and then removing trace amounts of $CHCl_3$ under vacuum for 12 h. This lipid mixture was hydrated with deionized distilled water. The quantity of water was chosen to make a ratio of PC/(PC + water) = 30 wt %. The mixture was placed under N_2 and freeze–thawed (−20°C to 55°C) 10 times, equilibrating each time for 10 min at 55°C (where isotropic CE and liquid-crystalline DPPC coexisted) to allow maximum incorporation of cholesterol. The sample was used for MAS NMR experiments soon after preparation.

Thoracic aorta tissue was obtained from New Zealand White rabbits fed with a cholesterol-rich diet (0.5% wt/wt cholesterol and 4% vol/wt peanut oil added to Purina rabbit chow) for 11 weeks. At the time of sacrifice, the cholesterol-fed rabbit used for these studies had a body weight of 3.6 kg and a plasma cholesterol level of 1270 mg/dl, much greater than the range in normal rabbits (50–70 mg/dl). Euthanasia was performed by administration of sodium pentobarbital and exsanguination according to a protocol approved by the Boston University Medical Center Institutional Animal Care and Use Committee. The lipid compositions of these lesions were measured after the NMR experiments by standard chemical analysis (Nolte et al., 1990), and the results are given in Tables 1 and 2.

NMR measurements

MAS NMR experiments were performed on a Bruker (Billerica, MA) AMX300 NMR spectrometer equipped with solid-state NMR accessories. Samples were held in 7-mm Zirconia rotors. A spherical Kel-F insert was used to cover the sample to prevent leakage and promote spinning. Total sample volume was ~100 μl. MAS NMR with high-power decoupling and without cross-polarization [direct polarization (DPMAS)] and MAS NMR with high-power decoupling and with cross-polarization (CPMAS) were used for identification of lipids in multiphase mixtures and the tissue samples. All spectra were obtained with a 5-μs 90° pulse width, 50-kHz spin-lock field and decoupling power, and a 5-s pulse interval. Typical CP contact time was 1 ms, with exceptions as indicated in the corresponding figures below. MAS spinning rates were 4.0–4.5 kHz for the crystalline samples and 1.5–2 kHz for the liquid and liquid-crystalline samples. The ^{13}C chemical shifts were referenced to the carbonyl carbon resonance of glycine [176.06 ppm from $(CH_3)_4Si$] as an external reference. Spectra were typically obtained over 2000^3 time-domain points and were zero filled to 8,192, giving a spectral digital resolution of ~2.0 Hz. All spectra were processed without line broadening unless otherwise noted. Sample temperatures were controlled to within 1°C with a Bruker B-VT-1000 variable-temperature unit. The probe temperature was calibrated as described previously (Guo and Hamilton, 1993, 1995a,b,c). Samples were allowed to equilibrate at the desired temperature for 15–20 min before data acquisition.

Differential scanning calorimetry

Experiments were carried out with a Perkin-Elmer DSC-7 instrument (Norwalk, CT). Samples (1.5–5 mg) were sealed in a stainless-steel pan. An empty pan was used as a reference sample. Heating and cooling rates were 5°C/min. The instrument was calibrated by use of the data obtained for high-purity standard material (indium).

X-ray powder diffraction

Patterns were recorded with nickel-filtered CuK-α radiation from an Elliot GX-6 rotating-mode generator (Elliot Automation, Borehamwood, UK) equipped with cameras using Franks double-mirror optics (Franks, 1958). The samples were packed into 1.0-mm-diameter Lindeman capillaries (Charles Supper, Natick, MA), sealed, and examined in variable-temperature sample holders. The sample–film distance was calibrated with the data of a standard material (crystalline cholesteryl myristate).

TABLE 1 Lipid mass (mg) of the rabbit aortic sections

	Sample					
	Dry tissue	Total lipid	CE	TG	CHOL	Phospholipid
Control	26.5	1.00	0.004	0.05	0.17	0.65
Lesion	29.1	6.77	2.82	0.25	1.61	1.73

The composition of the atherosclerotic lesion is similar to that of previously published compositions of lesions from CHOL-fed NZW rabbits (Nolte et al., 1990).

TABLE 2 Total mol % distribution of acyl chains of the rabbit aortic sections

	Sample				
	16:0	16:1	18:0	18:1	18:2
Control	31	21	19	26	3
Lesion	14.4	4.4	4.3	58.5	11.6

The acyl chain composition of the lesion sample served as a model for CE mixtures used in previous study (Guo and Hamilton, 1995) and in this study.

Microscopy

Experiments were performed on a Leitz-Dialux microscope fitted with a polarizer and heating stage 80 (Leitz/Wild, Burlington, MA). Photomicrographs were taken with a Nikon Microflex UFX camera system (Nikon, Inc., Garden City, NJ) with 35-mm film (Kodak Ektachrome ASA 200).

RESULTS AND DISCUSSION

^{13}C MAS NMR features of crystalline CHOL

Pure cholesterol can exist in three thermodynamically stable crystalline forms: monohydrate (ChM), low-temperature anhydrous (ChAl), and high-temperature anhydrous (ChAh). ChAl and ChM convert to ChAh at 38°C and 85°C, respectively. The CPMAS spectra of ChM, ChAl, and ChAh are shown in Figs. 1 *A*, 1 *B*, and 1 *C*, respectively. For comparison, a static sample spectrum of ChAh (obtained with the same experimental conditions but without spinning) is shown in Fig. 1 *D*. Without MAS, the spectrum was broad and featureless even after high-power decoupling and cross-polarization transfer were applied. With CPMAS, high-resolution spectra were obtained, and multiple signals of the same carbon representing the crystallographically inequivalent molecules were resolved for various carbon atoms, such as C5, C6, C3, C14/17, C9, and C18. Line widths as low as 10 Hz were observed, and peaks separated by as little as 0.2 ppm were resolved. Other steroid carbons

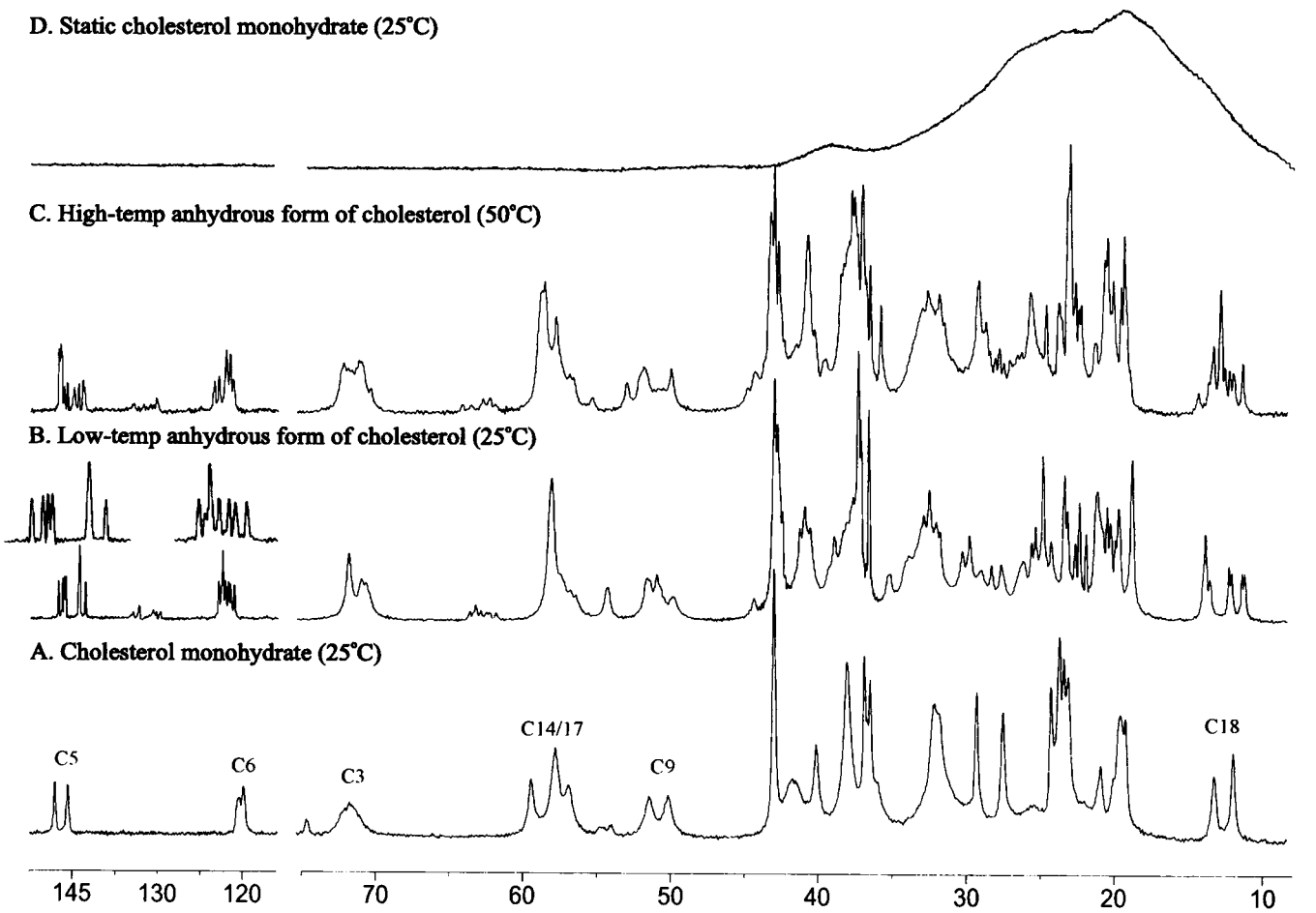

FIGURE 1 The ^{13}C CPMAS of (*A*) cholesterol monohydrate, (*B*) a low-temperature form of anhydrous cholesterol, (*C*) a high-temperature form of anhydrous cholesterol, and (*D*) the same sample as in (*C*) but without spinning. Selected CHOL resonances are identified by the standard numbering system for CHOL. The number of scans was 1000 for each spectrum.

might also give multiple signals, but they are superimposed in a relative small frequency region and thus are not well resolved from each other. The chemical shifts of selected carbons are listed in Table 3.

For ChM, carbons such as C5, C6, C9, and C18 had two peaks with approximately equal intensities (Fig. 1 *A*). In the crystalline structure of ChM the monohydrate molecules exist in bilayers, with the hydroxyl arranged in sheets through H-bonding (Craven, 1976, 1979). Although there are eight crystallographically different molecules in the unit cell, the shieldings on the molecules in each half of the bilayer are similar because of the sublattice pseudosymmetry (Craven, 1979). The observation of two sets of signals for C5, C6, and C18 reflects the inequivalent packing in the two halves of the bilayer. Only one broad but symmetric peak was observed for C3 (Fig. 1 *A*), because the shieldings on C3 in different molecules throughout the H-bonded network are not so distinctive. H-bonding also reduces the molecular motions of C3, resulting in line broadening.

In the crystal form ChAl, the C5, C6, C18, and C3 carbons each had multiple peaks with varying peak intensities (Fig. 1 *B*). For C5, a downfield group contained four well-separated peaks of approximately the same intensities (140.8–141.7 ppm), and an upfield group contained two peaks at 139.2 and 138.5 ppm (Table 3). The peak at 138.5 ppm has approximately the same intensity as each of those in the downfield group, whereas the peak at 139.2 ppm is approximately three times as intense. Thus, six nonequivalent signals for the C5 were resolved from the eight symmetrically inequivalent molecules in the single-crystal structure (Shieh et al., 1977). In addition, six peaks were well resolved for C6 and C18, five with nearly the same intensity and the other approximately three times as intense. With negative line broadening applied to the Fourier transform to enhance resolution, an additional small peak was revealed nearby the intense peak (Fig. 1 *B*, inset). For C3, one narrow downfield peak and one broad upfield peak were observed. According to the single-crystal data, the eight symmetrically inequivalent molecules are H-bonded in two separated chains parallel to each other (Shieh et al., 1977). Inasmuch as the chemical shift of C3 is affected by H-bonding, the observation of two different peaks for C3 suggests different molecular interactions near the polar headgroup between the two chains.

ChAl converts to ChAh at 38°C, and ChM to ChAh at 85°C. Both transitions were accompanied by significant spectral changes. The CPMAS spectra obtained for ChAh formed from the two crystals were the same (Fig. 1 *C*). In the C5 region, multiple peaks with slightly different chemical shifts were observed; peaks on the upfield have similar intensities, whereas the two most downfield peaks are much more intense. For C6, five peaks were observed, all slightly broader than those observed for the ChAl form, with two peaks in the middle approximately two to three times more intense. The C18 carbon also gave multiple peaks with a complicated intensity distribution. The C3 region consisted of a broad envelope of resonances. The phase transition from ChAl to ChAh is accompanied by the variation of the isooctyl chain conformations and the reorientation of the steroid rings, leading to a more complicated structure with 16 inequivalent molecules in the unit cell (Hsu and Nordman, 1983). Fig. 1 *B* and *C* reveals multiple resonances with varying intensities for C5, C6, and C18 carbons, corresponding to these molecular rearrangements. Although the x-ray powder diffraction patterns of ChAl and ChAh are rather similar (Loomis et al., 1979), the ^{13}C MAS NMR resonance features are significantly different for these two crystals, implying that MAS NMR is more sensitive to the changes in molecular arrangements in the crystalline structures.

In additional temperature studies, CPMAS spectra showed that ChAh formed by heating ChAl readily converted back to ChAl right below the phase transition (~38°C), whereas ChAh formed by heating ChM remained metastable at 25°C for >4 h before eventually converting to the ChAl crystalline form. On the other hand, ChM exposed to dry room atmosphere overnight gave a ^{13}C CPMAS spectrum the same as that of ChAl, implying complete dehydration, even though the crystals still had the platelike appearance characteristic of ChM morphology as viewed by the optical microscopy.

CHOL crystals under the polarizing microscope

Large crystals of ChM and ChAl grown under ideal conditions (solvent, concentration, and temperature) are well distinguishable by optical polarizing microscopy (Small, 1986). ChM has a platelike (Fig. 2 *A*) and ChAl a needlelike (Fig. 2 *C*) appearance. However, under nonideal conditions the identification by optical microscopy becomes ambiguous. For example, heating the crystals of ChAl or ChM converted them to ChAh at 38°C and 85°C, respectively. Because of the lack of a recrystallization medium, the newly formed ChAh were small, and the overall appearance was difficult to discern. Fig. 2 *B* shows the same view as Fig. 2 *A* after incubation of the crystal at 90°C for 3 h. The crystal seems to have broken into small pieces, but the morphology

TABLE 3 Chemical shifts (ppm) of C3, C5, and C6 resonances of pure CHOL in various crystalline forms

Crystal form	C3	C5	C6
ChM	71.8	142.4, 140.9	120.8, 120.3
ChAl	71.4, 70.6, 70.3	141.7, 141.2, 141.0, 140.8, 139.2, 138.5	122.9, 122.7, 122.5, 122.2, 121.8, 121.5, 121.1
ChAh	69.8–72.1	141.7, 141.4, 141.1, 140.7, 139.9, 139.3, 138.8, 138.6	123.4, 122.9, 122.1, 121.6, 121.2

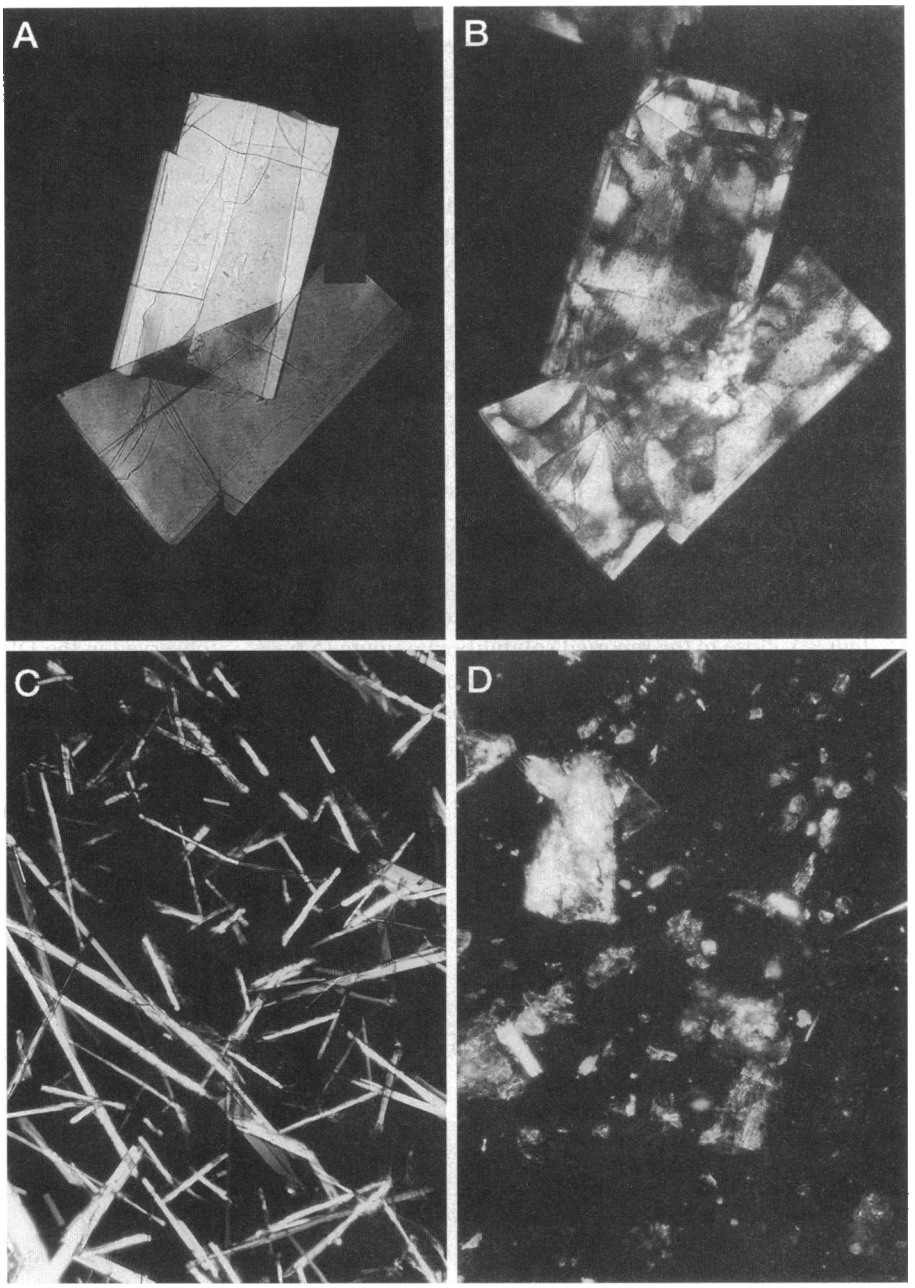

FIGURE 2 Photomicrograph (160×) of (*A*) cholesterol monohydrate recrystallized from an ethanol/water mixed solvent, (*B*) the same crystal dehydrated by incubation at 90°C for 2 h and then cooled to 25°C, (*C*) a low-temperature form of anhydrous cholesterol crystal recrystallized from diethyl ether, (*D*) a low-temperature form of anhydrous cholesterol crystal obtained directly from the manufacturer. The MAS NMR spectra of samples (*B*)–(*D*) at 25°C are identical (see Fig. 1 *B*).

of the newly formed ChAh is unclear. When the ChAl crystals shown in Fig. 2 *B* were heated to 50°C for 1 h, their appearance was not changed (not shown). Fig. 2 *D* shows the powdered cholesterol sample received from the manufacturer, which also does not reveal the crystalline structure. By MAS NMR this sample was identified as ChAl. Therefore, the application of optical microscopy for identification of crystalline forms of CHOL has significant limitations. In addition, when the crystallization occurs in biological samples the morphology will be further affected by many other influences, which could make the microscopy identification even more difficult. For example, needle-shaped crystals in CE-loaded macrophages had a melting point close to that of CHOL monohydrate (85°C). Electron micrographs showed membranes surrounding the crystals. Proof that these crystals were CHOL required their isolation and purification followed by TLC analysis (Tangirala et al., 1994).

Although x-ray diffraction can identify the different CHOL crystalline forms, the diffraction pattern contains overlapping data from all other coexisting structures when a complicated sample of mixed lipid species is present. Without purification and isolation, individual species and their corresponding structure might not be detected. However, with MAS NMR and with selected pulse programming conditions, both chemical composition and physical phases can be identified semiquantitatively without sample disruption (Guo and Hamilton, 1993, 1995a,c). The unique spectral features of CHOL in the three different crystalline

structures (Fig. 1) provide a basis for the identification of CHOL crystal forms in biological samples by MAS NMR.

MAS NMR of CHOL/CE mixtures

To study the interactions and physical states of CHOL in mixtures with CE, we incorporated anhydrous ChAl (24 wt %) into the model CE mixture for the rabbit atherosclerotic plaques (CE with CO/CP/CL = 69:17:14). The sample was mixed at 55°C, in the isotropic phase of CE, for at least 2 h before the NMR experiments to ensure that the solubilization of CHOL in CE oil reached equilibrium (Miller and Small, 1982). A DPMAS ^{13}C spectrum of this mixture at 60°C showed signals for isotropic CE and CHOL (Fig. 3A). Although most of the CHOL signals are superimposed with CE signals, the C3, C5, and C6 peaks are well separated and served to identify CHOL in the isotropic phase (Hamilton and Cordes, 1978) (Table 4). The peak intensity of CHOL/CE was 0.16 for the C5 and 0.15 for the C6 carbons, representing a solubility of CHOL in CE oil of ~13 mol % (5.2 wt %), close to the reported solubility maximum (5.6 wt %; North et al., 1978). The same proportion of CHOL/CE is found in the hydrophobic core of plasma high-density (Hamilton and Cordes, 1978) and low-density (Hamilton et al., 1979) lipoproteins. Higher temperatures did not result in significant changes in the relative peak intensities of CE and CHOL, whereas temperatures (51–55°C) near the crystalline–isotropic transition temperature of 50°C resulted in differential line broadening of the C5, C6, and C3 peaks of both CE and CHOL signals, as reported before (Hamilton et al., 1977).

TABLE 4 Chemical shifts (ppm) of C3, C5, and C6 resonances of CHOL in various lipid mixtures

Lipid Phase	C3	C5	C6
Isotropic CE	71.03	141.45	120.82
Sm CE	70.88	141.42	120.73
Isotropic CE with TO	71.09	141.43	120.84
Sm CE with TO	70.97	141.36	120.72
DPPC/CHOL bilayer	71.18	142.09	120.83

The peak intensity data of Fig. 3 *A* showed that the major portion of the CHOL in the mixture with CE was not observed in the DPMAS spectrum, which detects liquid and liquid-crystalline phases. To identify CHOL in the solid phase we carried out a CPMAS experiment to enhance

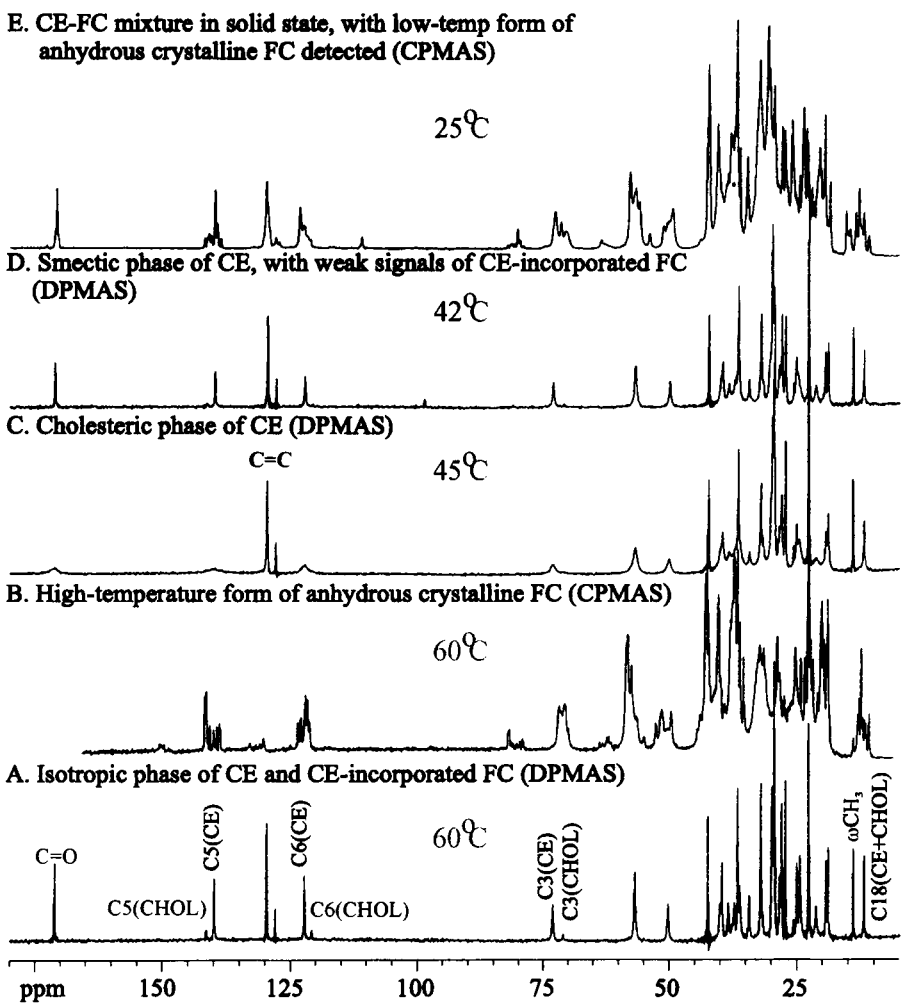

FIGURE 3 ^{13}C MAS NMR spectra of a binary mixture of CE and CHOL (24 wt % CHOL) at various temperatures: (*A*) isotropic phase at 60°C, (*B*) a high-temperature form of anhydrous crystalline cholesterol in coexistence with the isotropic phase at 60°C, (*C*) the cholesteric liquid-crystalline phase at 45°C, (*D*) the smectic liquid-crystalline phase at 42°C, and (*E*) a solid-state mixture of CE and CHOL at 25°C. The spectra in *A*, *C*, and *D* were obtained with DPMAS, and the spectra in *B* and *E* were obtained with CPMAS. Selected resonances are identified by the standard numbering system of the CHOL ring system and by C═O (CE), C═C (unsaturated carbons of oleic and linoleic acid), and ωCH_3 (terminal fatty acid CH_3). The number of scans was 4096 for each spectrum.

signals for solid components and to filter out the signals for liquid components (Guo and Hamilton, 1995a,c). The spectrum at 60°C (Fig. 3 *B*) was the same as that of ChAh (Fig. 1 *C*), indicating the excess CHOL is in a crystalline form that is indistinguishable from pure ChAh at this temperature. The spectrum in Fig. 3 *B* shows the ability of the CPMAS method to detect lipid in a crystalline state without interference from signals of lipids in the liquid state, the major phase of this mixture.

Temperature-dependent spectra between 50°C and 25°C showed that the solubilized CHOL had little effect on the phase behavior of the CE mixture, and the DPMAS spectra resembled those previously reported for CE without CHOL (Guo and Hamilton, 1993). When the sample was cooled, the cholesteric (Ch*) phase of CE was detected at 45°C (Fig. 3 *C*), and the smectic (Sm) phase at 42°C (Fig. 3 *D*). In both cases the coexisting crystalline CHOL was in the ChAh form, as detected by CPMAS (not shown). Direct detection of the small amount of CHOL solubilized in the Ch* liquid crystalline phase of CE was difficult because of the characteristic line broadening of the CE C5, C6, and C3 peaks in the Ch* phase (Guo and Hamilton, 1993). However, when the peaks became narrow again in the smectic phase, signals were observed for the C5, C6, and C3 peaks representing CHOL solubilized in the Sm phase, as manifested by their chemical shifts. On cooling the Sm phase to 25°C, the mixture solidified; the spectrum (Fig. 3 *E*) revealed a solid-state mixture of the low-temperature CHOL form (ChAl) and a solid solution of CE (Guo and Hamilton, 1993).

To study the solubilization of CHOL in the liquid-crystalline CE we replaced the CHOL component with CHOL containing ^{13}C enrichment at the C3 position. Incorporation of CHOL into the liquid-crystalline phases was clearly demonstrated by DPMAS (Fig. 4 *A-C*). The solubility of CHOL in the Sm phase was ~8 mol %, based on the relative peak intensities after correction for ^{13}C enrichment (Fig. 4 *C*), compared with 13 mol % in the isotropic phase (Fig. 4 *A*). Although line broadening in the Ch* phase precluded quantification of the CHOL solubility, the intense broad peak of CHOL centered at 72.5 ppm clearly indicated substantial incorporation of CHOL into the Ch* phase of CE (Fig. 4 *B*).

To our knowledge, direct detection of CHOL in liquid-crystalline CE phases has not been reported before. Results of Fig. 4 further demonstrate that the MAS NMR can readily and directly provide information on the chemical compositions in a liquid-crystalline phase, data that are difficult to obtain by other methods.

A mixture with the same CHOL/CE ratio as above, but with ChAl replaced by ChM, was prepared in the presence of excess water. The DPMAS spectra of the isotropic and liquid-crystal phases of this ChM/CE mixture were the same as those for the mixture with anhydrous CHOL (Fig. 3). Notably, the chemical shifts of CHOL C3, C5, and C6 carbons were identical in both cases (Table 3). This implies that the bound water molecule was lost when the ChM

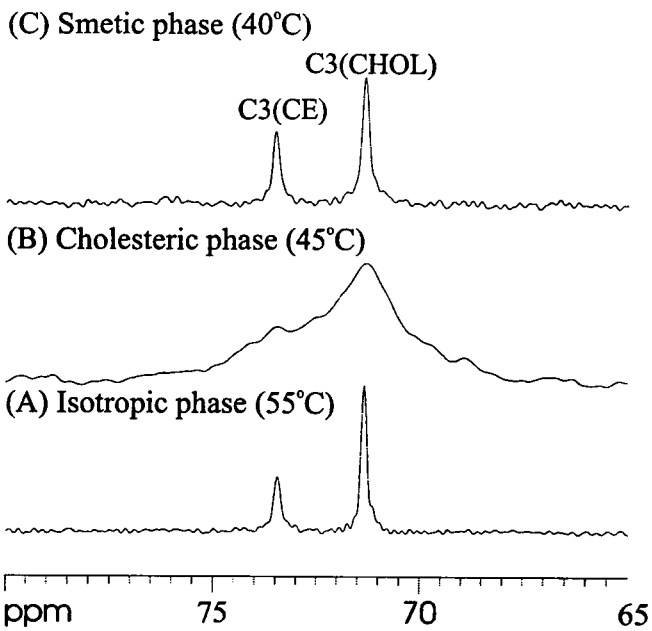

FIGURE 4 ^{13}C DPMAS spectra (60–80 ppm) of CE and CE-incorporated cholesterol with ^{13}C labeling at the C3 position. The number of scans was 800 for each spectrum.

dissolved in the hydrophobic CE oil. The pool of CHOL not dissolved in the CE oil was present as the monohydrate form, as shown by the characteristic spectrum (as in Fig. 1).

To assess whether the CE composition affects the solubility of CHOL, pure CO and a CO/CL (25 wt % CL) mixture were used for parallel studies as above. The results of MAS NMR experiments showed that these changes in the CE composition did not significantly affect the CE/CHOL interactions in the fluid phases (data not shown).

CHOL/CE/TO mixtures

Atherosclerotic plaques may contain small amounts of triglyceride (TG), which can significantly alter the phase behavior of the CE (Croll et al., 1985; Small, 1988). Levels of TG as low as 4 wt % remove the Ch* phase transition of the CE, and levels of >22% abolish all liquid-crystalline transitions (Hamilton et al., 1977). As a model system for plaques with TG, 10 wt % TO was added to the CE/CHOL mixture prepared as above. The melting point of the mixed system determined by MAS NMR (50°C) was 3°C lower than that for CE/CHOL without TO. The DPMAS spectrum of the isotropic phase at 60°C (Fig. 5 *A*) closely resembled that of the CE/CHOL mixture without TO (Fig. 3 *A*), except for the presence of peaks from the TO(1, 3) carbonyl and glycerol backbone carbons of TO. The TG(2) carbonyl is superimposed with the CE carbonyl signal. As revealed in the C5, C6, and C3 regions (Fig. 5 *A*), there was no significant enhancement of CHOL peaks relative to the CE peaks compared with the results shown in Fig. 3 *A*, implying that TO did not increase the solubility of CHOL in the isotropic phase. The crystal form of the coexisting excess CHOL

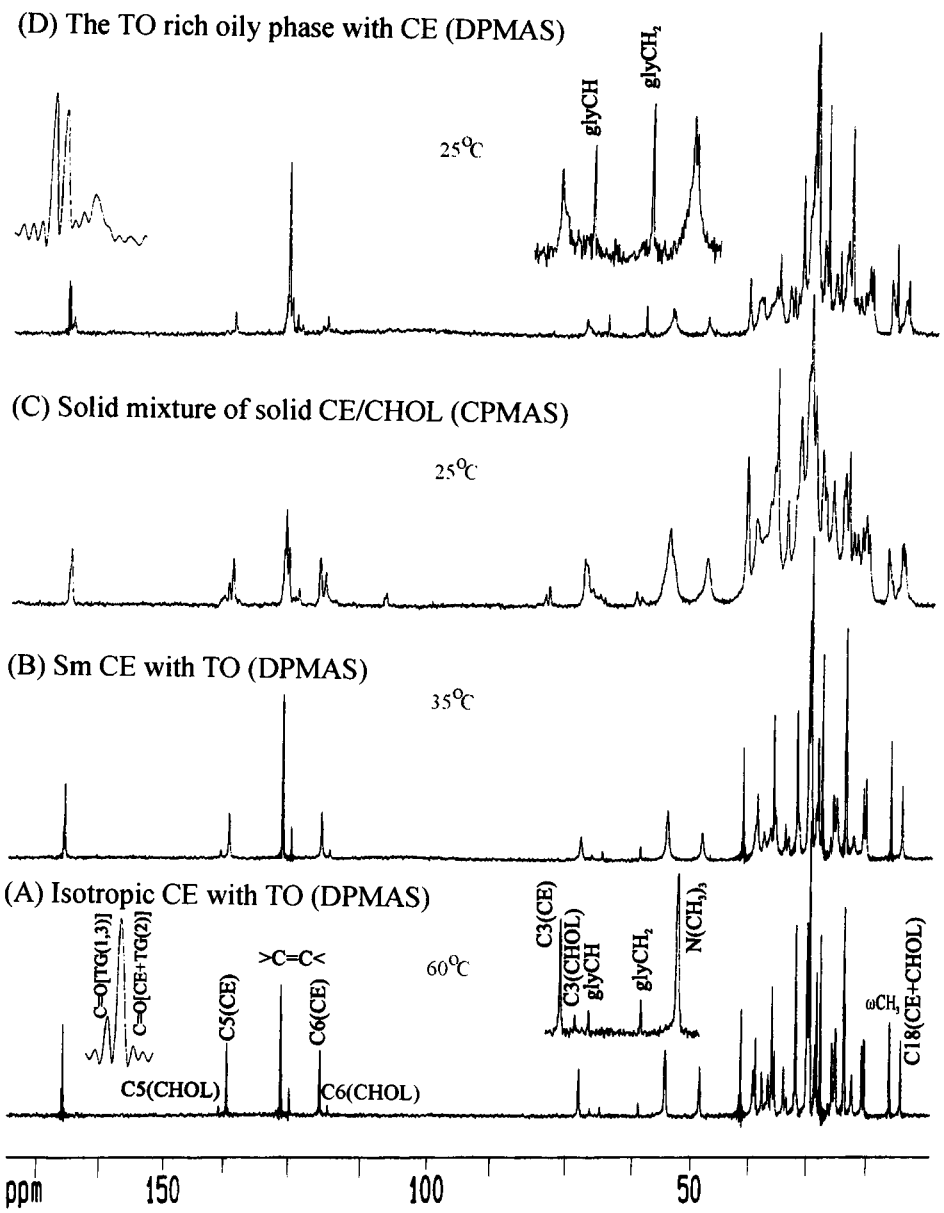

FIGURE 5 ^{13}C MAS NMR spectra of a ternary mixture of CE and CHOL and TO at various temperatures: (*A*) the isotropic phase at 60°C, (*B*) the Sm liquid-crystalline phase at 42°C, (*C*) a solid-state mixture of CE and CHOL at 25°C, and (*D*) TO oil in equilibrium with the solid mixture of CE and CHOL at 25°C. Spectra identifying liquid and liquid-crystalline phases [(*A*), (*B*), and (*D*)] were obtained with DPMAS, and that identifying the crystalline phases (*C*) with CPMAS. Resonances for the glycerol backbone of TO are designated glyCH and $glyCH_2$ in the expanded insets of (*A*) and (*D*). Other peaks are designated as in previous figures. The number of scans was 4096 for each spectrum.

(ChAh) was also unaffected by the TO, as indicated by the identity of the CPMAS spectrum (not shown) compared with that in Fig. 1 *B*.

On cooling, the isotropic phase transformed directly to the Sm phase at 43°C, and the Ch* phase was not observed, as reported (Hamilton et al., 1977). The integrated peak intensities in the DPMAS spectrum of the Sm phase (Fig. 5 *B*) gave a solubility of ~12 mol % of CHOL relative to CE, higher than the solubility without TO. Because interactions between CHOL and TO are rather weak (the solubility of CHOL in TO oil is only 0.5 wt %; Miller et al., 1982), TO might create structural defects in the CE Sm phase structure to accommodate solutes such as CHOL.

With further cooling to 25°C, the major portion of CE solidified to form a mixture of crystalline CE and amorphous CE (Guo and Hamilton, 1993), as indicated by the CPMAS spectrum (Fig. 5 *C*). To observe the fluid phases, we obtained a DPMAS spectrum of this mixture (Fig. 5 *D*). Narrow signals from the carbonyl and glycerol carbons of TO were readily observed, and a narrow C═O from CE was also observed downfield from a broad C═O signal representing the solid state (Fig. 5 *D*, *inset*). The narrow peaks in Fig. 5 *D* probably represent a separate TO-rich oil phase, containing some CE and coexisting with the solid CE/CHOL phase.

Following similar experimental protocols, by varying CHOL from anhydrous to monohydrate and substituting CO or CO/CL (25 wt % CL) for the CE mixture we showed that the solubility of CHOL in the isotropic and Sm phases of CE was not significantly affected by the change of CE composition or the hydration state of CHOL. The crystalline

forms of CHOL (ChAl, ChAh, and ChM) were also not affected by the addition of TO in any of the mixtures.

CHOL/CE/phospholipid mixtures

Lipids deposited in atherosclerotic plaques originate in part from low-density lipoproteins, triglyceride-rich remnant lipoprotein, and Lp(a) that contain phospholipid in addition to CE, CHOL, and TG (Bottalico et al., 1993; Small, 1988; Hamilton et al., 1978). In addition, the lipids in plaques are in a tissue environment that contains cell membrane, whose predominant lipids are phospholipids and CHOL. The interactions of CHOL and phospholipids in a bilayer system were recently characterized in a detailed multinuclear solid-state NMR study of DPPC/CHOL mixtures (Guo and Hamilton, 1995c). To complete our investigations of the model systems for plaques, we studied three samples that comprised phospholipids, CHOL, and CE, with the following mol % composition: CHOL/CEl/eggPC = 1:1:1; CHOL/CEl/DPPC = 1:1:1; and 2:1:1. All samples were hydrated above their gel-to-liquid-crystalline phase transition temperature in excess water. With the chosen CHOL contents, both eggPC and DPPC exist in a liquid-crystalline state at 25°C (McMullen et al., 1993), and CHOL can incorporate into the bilayer up to a 1:1 mol ratio (Bourges et al., 1967; Philips, 1990; Guo and Hamilton, 1995c). The phase diagrams (Bourges et al., 1967) further predicted that CE and unincorporated CHOL would be in a solid state at this temperature. In accord with predictions, the DPMAS spectrum (not shown) of each of these samples resembled published spectra of liquid-crystalline phospholipid/CHOL multilayers (Forbes et al., 1988; Guo and Hamilton, 1995c). The coexisting solid-state CE or CHOL was not detected. Under the experimental conditions used there were no significant spectral differences between eggPC/CHOL and DPPC/CHOL mixtures, except for the presence of the signals reflecting the chain unsaturation of eggPC. Because eggPC is less stable at elevated temperature, we substituted DPPC for eggPC to perform temperature-dependent studies. In a CHOL/CE/DPPC (1:1:1) mixture at 60°C, CE melted to form an isotropic phase and was detected in the DPMAS spectrum by the characteristic C=O, C5, C6, and C3 resonances (Fig. 6A). The C5 and C6 peaks of CHOL were broader than the corresponding CE peaks, a factor that may

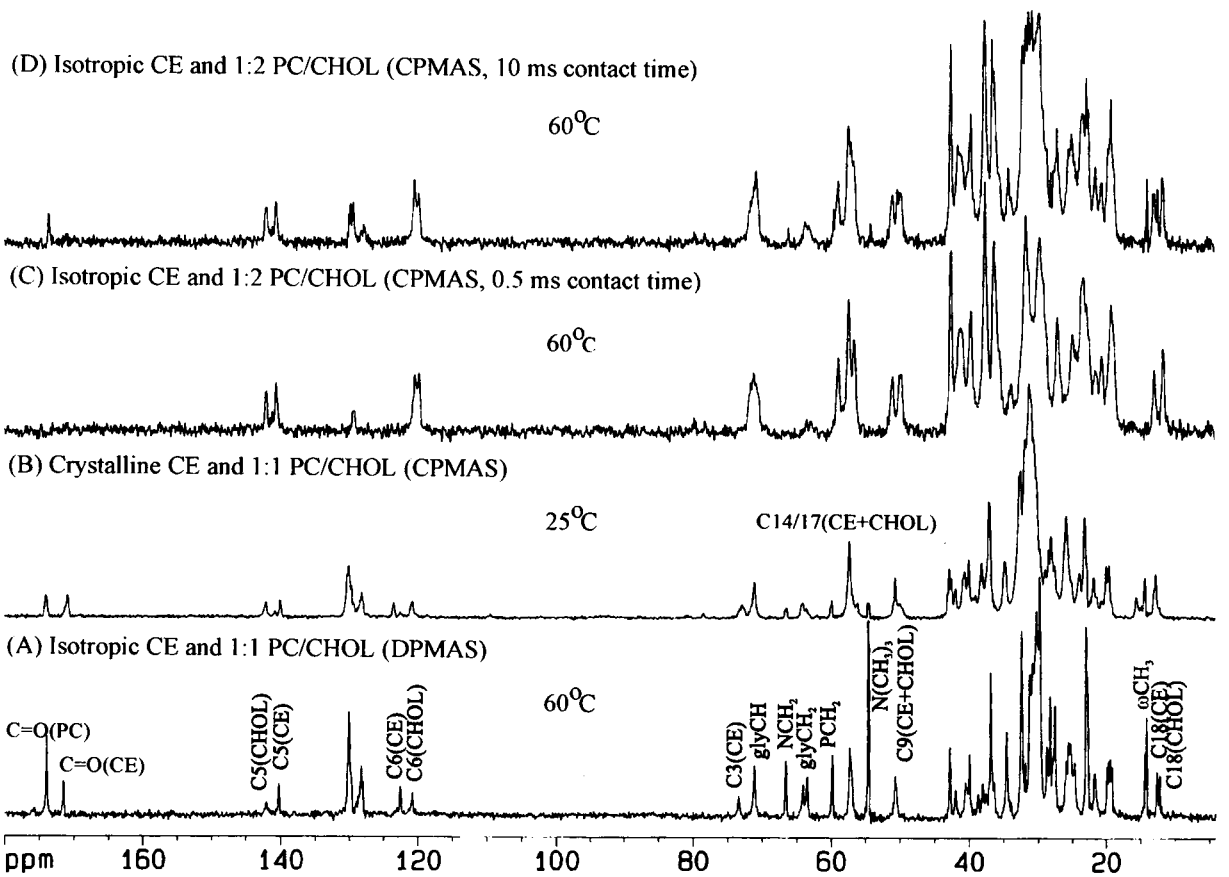

FIGURE 6 ^{13}C MAS NMR spectra of mixtures of CE and CHOL and phospholipids: (*A*) a liquid-crystalline eggPC/CHOL bilayer and isotropic CE at 60°C; (*B*) a solid-state mixture of CE and a liquid-crystalline DPPC/CHOL bilayer; (*C*) a crystalline CHOL monohydrate at 60°C in coexistence with DPPC/CHOL bilayers and isotropic CE, this spectrum obtained with a 0.5-ms cross-polarization contact time; and (*D*) the same as in (*C*) but with 10-ms contact time. Spectrum (*A*) was obtained with DPMAS, and spectra (*B*), (*C*), and (*D*) were obtained with CPMAS. The number of scans was 4096 for each spectrum.

hinder detection of CHOL in tissues (see below). The second model mixture with DPPC contained excess CHOL (CHOL/CE/DPPC = 2:1:1) and is predicted to have a bilayer phase comprising mainly DPPC and CHOL, a crystalline phase of CHOL, and a liquid or solid phase (temperature dependent) of CE with some CHOL (Bourges et al., 1967). The CPMAS spectrum at 25°C showed the coexistence of liquid-crystalline DPPC/CHOL with solid-state CE and ChM (Fig. 6 *B*). Because most of the CHOL signals are superimposed with CE signals, the spectral features of ChM were not clear in this spectrum. When the CE phase was melted, the CE signals were fully suppressed from the CPMAS spectrum. At 60°C, when we used a short contact time (0.5 ms) to attenuate the mobile DPPC/CHOL bilayer signals, the CPMAS spectrum (Fig. 6 *C*) was dominated by signals of crystalline ChM, and the liquid-crystalline signals were largely undetected, except for the peak from the main acyl chains at ~30 ppm. A CPMAS spectrum with a longer contact time (10 ms), which allows the cross-polarization transfer between nuclei with moderate or weak dipolar coupling (the bilayer phase), showed both ChM and a liquid-crystalline DPPC/CHOL phase (Fig. 6 *D*). Thus, by varying the contact time, one can observe either the crystalline phase alone or both crystalline and liquid-crystalline phases.

In the fluid phases (liquid-crystalline and isotropic) most of the steroid and isooctyl carbons of CE and CHOL were superimposed, but well-separated peaks were observed for C5, C6, C18, and C3 (Fig. 6 *A*). Also, separate fatty acyl ωCH_3 peaks were observed for CE and PC. The CE signals in Fig. 6 *A* were identified by the characteristic chemical shifts of CE (Guo and Hamilton, 1993) and also by comparison with the spectrum of DPPC/CHOL multibilayers without CE signals (Guo and Hamilton, 1995c). The solubility of CE in hydrated liquid-crystalline phospholipid is expected to be very small (Hamilton et al., 1983; Spooner et al., 1986), and signals from this pool of CE were not observed.

Spectral features of rabbit arterial tissues

By making use of the data from model systems and the protocols developed to monitor different phases and chemical constituents in lipid mixtures, we studied the lipids in atherosclerotic plaques dissected from cholesterol-fed New Zealand White rabbits. Such plaques serve to test our protocol for distinguishing different phases before application of the method to human plaques. They are also particularly suitable samples for MAS NMR experiments because most of the CE are not melted at body temperature (Nolte et al., 1990) and conventional ^1H NMR spectra show severely broadened signals unless high temperatures are used (Kroon et al, 1982).

As a control sample, a segment of normal aortic tissue without visible plaques was studied. The DPMAS spectrum at 37°C showed only weak signals from plasma membranes and mobile groups on proteins (Fig. 7 *A*). For a segment of aortic tissue with observable plaques, the spectrum without MAS was dominated by TG signals (Fig. 7 *B*). Although a weak signal at 54.3 ppm was seen from the choline methyl groups of choline-containing phospholipids, the prominent signals characteristic of TG (carbonyl and glycerol) suggest that most of the acyl chain signals are contributed by TG. This spectrum, which is the same as would be obtained by conventional high-resolution NMR, suggests that most of the CE is not in a liquid phase at 37°C and thus is not mixed with the TG (see below).

In the DPMAS spectrum (Fig. 7 *C*) numerous narrow steroid ring signals were observed. The chemical shifts of the C═O, C═C, C5, C6, C3, and C18 are characteristic of CE in a liquid-crystalline phase. Signals from CHOL and other lipids are not detected. To investigate possible coexisting solid-state lipid components, we used CPMAS to enhance signals from solid phases and simultaneously suppress signals from liquid and liquid-crystalline phases (see Fig. 6). The spectrum (Fig. 7 *D*) showed significant steroid ring carbon signals; the absence of TG signals showed that noncrystalline phases were well suppressed. The unsaturation revealed in the olefinic region shows a single signal characteristic of oleic acid, and the signal from linoleic groups seen in the spectra of both Fig. 7 *B* and 7 *C* is not seen. The observation of the oleoyl chain suggested that the steroid signals observed in Fig. 7 *D* originated from CE mixtures. When this sample was heated to 47°C, the signals for the solid lipid largely disappeared (spectrum not shown), confirming that the solid phase observed in Fig. 7 *D* was mainly a CE solid solution. Some crystalline CHOL may contribute to the spectrum in Fig. 7 *D* and be largely obscured by the CE signal (see below).

It is important to note that the present spectra represent significant improvements in detection of plaque lipids, as judged by the CE component. The DPMAS spectrum of CE in the rabbit plaque containing 2.8 mg of CE (Fig. 7 *C*) shows signal-to-noise ratios comparable with those of a conventional NMR spectrum of a human plaque containing 26 mg of CE and obtained in approximately the same time period (Hamilton et al., 1979). Unesterified cholesterol was not detected in the MAS NMR spectra of rabbit plaques. Although the plaque sample (Table 2) contained an equimolar ratio of CHOL and CE (CHOL/CE/phospholipid = 2:2:1, in moles), several factors effectively dilute the CHOL signals relative to CE signals. The structural environments of CHOL are more heterogeneous than is CE. The pools of CHOL include the lamellar phase of cell membranes and phospholipids deposited in the plaque, crystals, CE solubilized, and possibly protein bound (Small, 1988). Moreover, the model mixture of 1:1:1 CHOL/CE/PC (Fig. 6 *A*) showed broadening of CHOL resonances in the lamellar phase (e.g., C5 and C6) relative to the corresponding CE resonances. Comparison of the choline methyl resonance in the plaque spectrum (Fig. 7 *C*) and in the model system spectrum (Fig. 6 *A*) shows a greatly reduced choline signal from the tissue. Based on this signal, the signals for CHOL in the bilayer

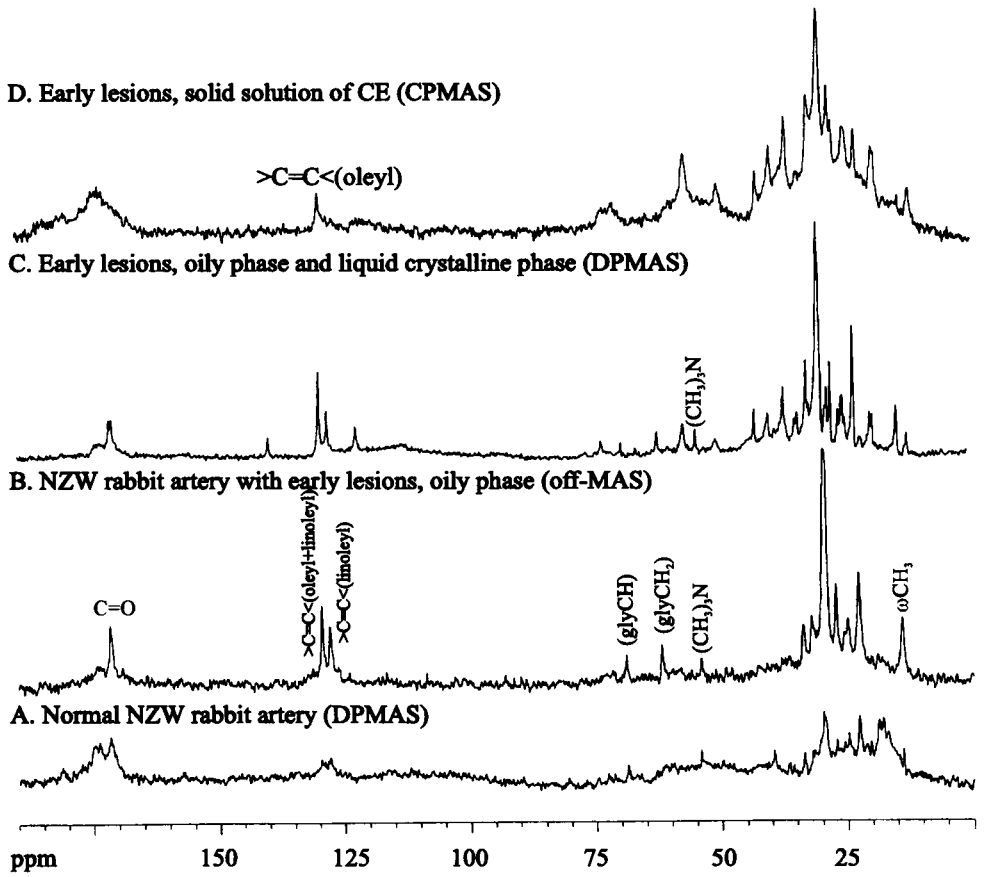

FIGURE 7 ^{13}C MASNMR spectra of an atherosclerotic plaque dissected from a CHOL-fed rabbit: (*A*) MAS NMR spectrum of a normal rabbit artery, (*B*) the oily phase of a rabbit plaque detected by off-magic angle spinning, (*C*) the oily phase and the liquid-crystalline phase in the plaque detected by DPMAS, and (*D*) the solid phase of the plaque composed mainly of CE mixtures obtained by CPMAS. The number of scans was 12,288 for each spectrum. All spectra were obtained at 37°C.

phase would be too weak to be observed. The signal-to-noise ratio in the plaque spectrum is also too low for CHOL dissolved in CE to be observed, and, as shown above (Fig. 3 *C* and *D*), the solubility of CHOL in liquid CE is reduced in liquid-crystalline CE. The amount of CHOL in this sample that is possibly crystalline (<1 mg) is likely also too small to be detected. Although signals of the crystalline CHOL would be enhanced by CP, the splitting of signals (e.g., C5, C6, and C18) decreases the signal-to-noise ratio relative to that of CE. In recent studies of human plaques containing much higher total amounts of CHOL/mg of tissue and higher CHOL/phospholipid ratios, CPMAS spectra have revealed crystalline CHOL in the monohydrate form (Hamilton et al., 1996).

These spectra of rabbit plaques provide more details about the organization and phase behavior than do previous NMR studies, which observed only the liquid phase above body temperature (Kroon et al., 1982). Our observation that CE is present in liquid-crystalline and solid states at the same temperature indicates the coexistence of heterogeneous lipid pools: pools rich in cholesteryl linoleate remained in the liquid-crystalline state, whereas pools rich in cholesteryl oleate and saturated esters solidified. In some atherosclerotic plaques, minor plaque lipid components such as triglycerides may lower the liquid-to-liquid-crystalline phase transition temperature and may also prevent crystallization of CE. The phase behavior of the cholesteryl esters in our sample, as reflected in the spectra of Fig. 7 *C* and *D*, shows that little of the observed triglyceride (Fig. 7 *B*) was co-mixed with the CE in plaques. Such triglyceride can exist as fat cells outside the actual plaque. A similar observation was made for human atherosclerotic plaque (Hamilton et al., 1978). The spectra obtained of rabbit arterial lesions demonstrate the feasibility of the MAS NMR protocol for enhanced detection of lipids in intact human plaques.

SUMMARY

Free cholesterol, cholesteryl esters, triglyceride, and phospholipids are the important lipid components of human atherosclerotic lesions. Depending on the lipid composition and the sample temperature, the lipid components can exist in crystalline, liquid-crystalline, or isotropic phases. A solid-state NMR with magic-angle-sample spinning protocol has been developed to study the crystalline structures of free cholesterol, the molecular interactions of cholesterol with other lipids in both the liquid-crystalline state and the isotropic state, and the simultaneous identification of coexisting multiphases of individual lipid species. Based on the results of model systems, an early atherosclerotic lesion from New Zealand White rabbit arterial tissue was investigated, and various lipid components and the corresponding phases were identified.

We thank Dr. Richard Cohen for supplying the rabbit aortic tissue.

This research was supported by grants RO1 HL41904 to J.A.H. and AHA13434945 to W.G.

REFERENCES

Bottalico, L. A., G. A. Keesler, G. M. Fless, and I. Tabas. 1993. Cholesterol loading of macrophages leads to marked enhancement of native lipoprotein(a) and apoprotein(a) internalization and degredation. *J. Biol. Chem.* 268:8569–8673.

Bourges, M., D. M. Small, and D. G. Dervichian. 1967. Biophysics of lipidic association. II. The ternary systems: cholesterol-lecithin-water. *Biochim Biophys Acta.* 137:157–167.

Craven, B. M. 1976. Crystal structure of cholesterol monohydrate. *Nature (London).* 260:727–729.

Craven, B. M. 1979. Pseudosymmetry in cholesterol monohydrate. *Acta Crystallogr.* B35:1123–1128.

Croll, D. H., D. M. Small, and J. A. Hamilton. 1985. Molecular motions and thermotropic phase behavior of cholesteryl esters with triolein. *Biochemistry.* 24:7971–7980.

Forbes, J., C. Hust, and E. Oldfield. 1988. High-field, high resolution proton "magic angle" sample spinning nuclear magnetic resonance spectroscopic studies of gel and liquid crystalline lipid bilayers and the effects of cholesterol. *J Am. Chem. Soc.* 110:1059–1065.

Franks, A. 1958. Some developments and applications of microfocus x-ray diffraction techniques. *Br. J. Appl. Phys.* 9:349–352.

Guo, W., and J. A. Hamilton. 1993. Molecular organization and motions of cholesteryl esters in crystalline and liquid crystalline phases: a ^{13}C and ^{1}H magic angle spinning NMR study. *Biochemistry.* 32:9038–9052.

Guo, W., and J. A. Hamilton. 1995a. Phase behavior and crystalline structures of cholesteryl ester mixtures: a ^{13}C MASNMR study. *Biophys. J.* 68:2376–2386.

Guo, W., and J. A. Hamilton. 1995b. Molecular organization and motions of crystalline monoacylglycerols and diacylglycerols: a C-13 MASNMR study. *Biophys. J.* 68:1383–1395.

Guo, W., and J. A. Hamilton. 1995c. Multinuclear solid state NMR study of phospholipid-cholesterol interactions, dipalmitoylphosphatidylcholine-cholesterol binary system. *Biochemistry.* 34:14,174–14,184.

Hamilton, J. A., and E. H. Cordes. 1978. Molecular dynamics of lipids in human plasma high density lipoproteins, a high field ^{13}C NMR study. *J. Biol. Chem.* 253:5193–5198.

Hamilton, J. A., E. H. Cordes, and C. J. Clueck. 1979. Lipid dynamics in human low density lipoproteins and human aortic tissue with fibrous plaques. *J. Biol. Chem.* 254:5435–5441.

Hamilton J. A., K. W. Miller, and D. M. Small. 1983. Solubilization of triolein and cholesteryl oleate in egg phosphatidylcholine vesicles. *J. Biol. Chem.* 258:12,821–12,826.

Hamilton, J. A., J. Morrisett, M. E. BeBakey, G. M. Lawrie, and W. Guo. 1996. Detection of crystalline cholesterol in human atherosclerotic tissue by magic angle spinning (MAS) NMR. *Biophys. J.* 70:A90-Su-Pos332.

Hamilton, J. A., N. Oppenheimer, and E. H. Cordes. 1977. Carbon-13 nuclear magnetic resonance studies of cholesteryl esters and cholesteryl ester/triglyceride mixtures. *J. Biol. Chem.* 252:8071–8080.

Hsu, L.-Y., and C. E. Nordman. 1983. Phase transition and crystal structure of the 37 C form of cholesterol. *Science.* 220:4–6.

Kodali, D. R., D. M. Small, J. Powell, and K. Krishnan. 1991. Infrared micro-imaging of atherosclerotic arteries. *Appl. Spectrosc.* 45: 1310–1317.

Kroon, P. A., D. M. Quinn, and E. H. A Cordes. 1982. Carbon-13 nuclear magnetic resonance study of aortic lesions and cholesteryl ester rich lipoproteins from atheroslcerotic rabbit. *Biochemistry.* 21:2745–2753.

Loomis, C. R., G. G. Shipley, and D. M. Small. 1979. The phase behavior of hydrated cholesterol. *J. Lipid Res.* 20:525–536.

McMullen, T. P., R. N. Lewis, and R. N. McElhaney. 1993. Differential scanning calorimetric study of the effect of cholesterol on the thermotropic phase behavior of a homologous series of linear saturated phosphatidylcholines. *Biochemistry.* 32:516–522.

Miller, K. W., and D. M. Small. 1982. The phase behavior of triolein, cholesterol and lecithin emulsions. *J. Coll. Surf. Sci.* 89:466–478.

Nolte, C. J. M., A. T. Tercyak, H. M. Wu, and D. M. Small. 1990. Chemical and physicochemical comparison of advanced atherosclerotic lesions of similar size and cholesterol content in cholesterol-fed New Zealand white and Watanabe Heritable hyperlipidemic rabbits. *Lab. Invest.* 62:213–222.

North, B. E., S. S. Katz, and D. M. Small. 1978. The dissolution of cholesterol monohydrate crystals in atherosclerotic plaque lipids. *Atherosclerosis.* 30:211–217.

Phillips, M. C. 1990. Cholesterol packing, crystallization, and exchange properties in phosphatidylcholine vesicle systems. *Hepatology.* 12: 75S–82S.

Shieh, H. S., L. G. Hoard, and C. E. Nordman. 1977. Crystal structure of anhydrous cholesterol. *Nature (London).* 267:287–290.

Small, D. M. 1986. Handbook of Lipid Research: The Physical Chemistry of Lipids: From Alkanes to Phospholipids. Plenum Publishing Corp., New York. Chap. 11.

Small, D. M. 1988. George Lyman Duff Memorial Lecture. Progression and regression of atherosclerotic lesions. Insights from lipid physical biochemistry. *Arteriosclerosis.* 8:103–129.

Spooner, P. J. R., J. A. Hamilton, D. L. Gantz, and D. M. Small. 1986. The effect of free cholesterol on the solubilization of cholesteryl oleate in phosphatidylcholine bilayers: a ^{13}C NMR study. *Biochem. Biophys. Acta.* 680:345–353.

Spooner, P. J. R., and D. M. Small. 1987. Effect of free cholesterol on incorporation of triolein in phospholipid bilayers. *Biochemistry.* 26: 5820–5825.

Tangirala, R. K., W. G. Jerome, N. L. Jones, D. M. Small, W. J. Johnson, J. M. Glick, F. H. Mahlberg, and G. H. Rothblat. 1994. Formation of cholesterol monohydrate crystals in macrophage-derived foam cells. *J. Lipid Res.* 35:93–104.

Toussaint, J.-F., J. F. Southern, V. Fuster, and H. L. Kantor. 1994. C-13 NMR spectroscopy of human atherosclerotic lesions: relation between fatty acid saturation, cholesteryl ester content, and luminal obstruction. *Arterioscler. Thromb.* 14:1951–1957.